A strategy of the longitudinal control for the tandem wing configuration design

Marcin Figat
The Aircraft Design Division, Faculty of Power and Aeronautical Engineering, Warsaw University of Technology, Warsaw, Poland

Abstract

Purpose – This paper presents first sight on the longitudinal control strategy for an aircraft in the tandem wing configuration. It is an aerodynamic strongly coupled configuration that needs a lot of detailed aerodynamic analysis which describes the mutual impact of the main parts of the aircraft. The purpose of this paper is to build the numerical model that allows to make an analysis of necessary flaps (front and rear) deflection and prepare the control strategy for this kind of aircraft.

Design/methodology/approach – Aircrafts' aerodynamic characteristics were obtained using the MGAERO software which is a commercial computing fluid dynamics tool created by Analytical Methods, Inc. This software uses the Euler flow model. Results from this software were used in the static stability evaluation and trim condition analysis. The trim conditions are the outcome of the optimisation process whose goal was to find the best front and rear flap deflection to achieve the best lift to drag (L/D) ratio.

Findings – The main outcome of this investigation is the proposal of strategy for the front and rear flap deflection which ensured the maximum L/D ratio and satisfied the trim condition. Moreover, the analysis of the mutual impact of the front and rear wings and the analysis of the control surface impact on the aerodynamic characteristic of the aircraft are presented.

Research limitations/implications – In terms of aerodynamic computation, MGAERO software uses an inviscid flow model. However, this research is for the conceptual stage of the design and the MGAERO software grantee satisfied accurate respect to relatively low time of computations.

Practical implications – The ultimate goal is to build an aircraft in a tandem wing configuration and to conduct flying tests or wind tunnel tests. The presented result is one of the milestones to achieve this goal.

Originality/value – The aircraft in the tandem wing configuration is an aerodynamic-coupled configuration that needs detailed analysis to find the mutual interaction between the front and rear wings. Moreover, the mutual impact of the front and rear flaps is necessary too. Obtaining these results allowed this study to build the numerical model of the aircraft in the tandem wing configuration. It allows to find the best strategy of flap deflection, which allows to obtain the maximum L/D ratio and satisfy the trim condition.

Keywords Tandem wing, Aerodynamic design, Trim conditions, Optimisation, CFD

Paper type Research paper

Introduction

From the beginning of aviation until now, aircraft are designed and built in many different configurations (Roskam and Lan, 1997; Gudmundsson, 2014; Raymer, 2018; Scholz, 2015; Kundu, 2019; Chudoba, 2019; Stinton, 2001). The search and testing of new arrangements of the aircraft were always associated with the need for improvement of the newly designed aircraft performance. For years, some configurations became more popular, but some not. It is caused because every configuration generates the various set of challenges and problems. Almost always they are associated with aerodynamic coupling which may significantly impact the main aircraft's geometrical features like a wing, fuselage and empennage.

Generally, in terms of the configurations, aircraft are divided into two main groups (Scholz, 2015): conventional and unconventional. The definition of conventional configuration assumes that an aircraft has a fuselage, a wing and an empennage placed at its rear end. This is the typical configuration of airliners, especially popular for big commercial transportation. The other configurations, which do not satisfy the conventional criterion, are called unconventional. This is a group of military or special-purpose aircraft. A lot of small light aircraft are built in unconventional configurations too. Moreover, it should be mentioned that the first flying powered aircraft was built in unconventional configuration – the biplane in canard configuration (Hallion, 2019).

The group of unconventional configurations of aircraft is quite large and miscellaneous (Goetzendorf-Grabowski and Mieloszyk, 2016; Schmitt, 2001). Contains many different designs like multi-wing configuration (biplane, triplane and tandem wing) (Roedts, 2009; Westin and Pinto, 2008; Jones *et al.*, 2015), canard configuration (Rizzi *et al.*, 2011; Goetzendorf-Grabowski and Goraj, 1987), three surfaces

The current issue and full text archive of this journal is available on Emerald Insight at: **https://www.emerald.com/insight/1748-8842.htm**

Aircraft Engineering and Aerospace Technology
95/1 (2023) 155–169
Emerald Publishing Limited [ISSN 1748-8842]
[DOI 10.1108/AEAT-12-2021-0372]

Received 4 February 2022
Revised 9 May 2022
Accepted 8 June 2022

configuration (Goetzendorf-Grabowski and Antoniewski, 2016), etc. The division within the group of the unconventional aircraft may be defined in many different ways. It may be associated with the kind of main parts of the aircraft, their position and their number but maybe classified in terms of lift force generation methods and/or methods to obtained static stability too.

This paper presents the analysis of a tandem wing configuration, which belongs to the group of unconventional configurations. Firstly, the comparative analysis in terms of the method of lifting force generation and obtaining longitudinal stability was made. To do this three configurations were chosen: conventional, canard and tandem wing. Figure 1 presents those three main aircraft's layouts.

The first and the most popular is a conventional configuration [Figure 1(a)] (Roskam and Lan, 1997; Gudmundsson, 2014). The necessary lift is produced by the main wing only, while the horizontal stabiliser is designed to control and to obtain longitudinal stability only. The wing's impact of the tail is measured by a downwash angle, which significantly affects the aerodynamic efficiency of the horizontal stabiliser. As was mentioned, this configuration is the most popular in nowadays aviation.

The second configuration [Figure 1(b)] is a canard configuration, where the empennage is placed in the front of the main wing. In this configuration, the canard ensures both longitudinal stability and control but may have a significant impact on the main wing. The disturbance generated by the canard may considerably influence on the main wing performance and reduces the lift on the wing. The most famous aircraft designed in this configuration is the first aircraft – the Wright brothers Flyer I (Hallion, 2019).

Finally, the last and the least popular configuration is a tandem wing. It is the most coupled aerodynamic system from all presented configurations. It consists of two similar wings with almost the same span and chord. Both wings are responsible for lift generation, and both wings may play the role of the empennage (both wings may be equipped with the flaps that can be used as a control surfaces). The main feature of the tandem wing configuration is a reduction of the induced drag (Stinton, 2001) caused by the mutual impacts of both wings (Chou *et al.*, 2013; Cheng *et al.*, 2021). According to Munk's span factor, the lowest induced drag is going to be achieved for two wings placed on the same level and the wing's stagger (gap-to-chord ratio) equal to 1 (Munk, 1922) . Moreover, one of the additional advantage is a very low take-off and landing velocity, thanks to higher lift because of installation high lift devices on both wings. A great enthusiast of the tandem wing configuration was Sir Herbert Miles (Brinkworth, 2016), who built an experimental fighter aircraft M.35 and M.39B in tandem wing configuration. The most famous aircraft are Quicke, Proteus (Proteus, 2021) and ATTT133 (Figure 2). Nowadays, this configuration is often used to design the unmanned aircraft vehicle (UAV) for military purposes.

In terms of the aerodynamic interaction all presented above aircraft's configurations gives simple conclusions. The conventional configuration has the least aerodynamic coupling, so it is convenient to design. On the other hand, the configuration with the highest level of aerodynamic coupling, like a tandem wing or some unconventional design like modular airplane system (Kwiek, 2016), needs much more time to be designed (Goetzendorf-Grabowski and Figat, 2017). For such a design, all aerodynamic analyses should be made for complete aircraft configuration; a superposition method (Nelson, 1998; Phillips, 2004; Goraj, 2014) is not appropriate because analysis of each wing separately gives a significant error.

Therefore, the main goal of this paper is to identify the aerodynamic characteristic of the aircraft in tandem wing configuration. To examine and for analysis of the aerodynamic impact of the front wing on the rear wing to quantify of their mutual impact. Furthermore, the analysis of the impact of both flap deflection on the aerodynamic coefficient of the aircraft is shown. And finally, the longitudinal control strategy which satisfies the trim condition and obtains the maximum possible L/D ratio is presented. The fulfilment of the trim condition is very important with respect to the strong impact of both wings.

Basic consideration

The research was conducted on the prepared model (Figure 3). The model for the numerical analysis consists of the fuselage, the front and the rear wing. Both wings were placed on the same level. The high wing configuration with the wing with the same aerofoil without any aerodynamic and geometric twist was chosen. The incidence angle of the wing was applied only for the rear wing. It was assumed to be equal to 3 degrees. Only a single case of the wings position (wings stagger $\Delta s = 1.5$) was considered.

Figure 1 Typical aircraft configuration

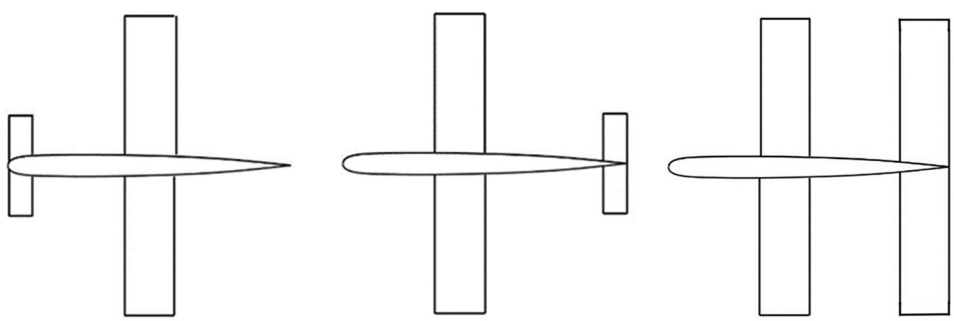

Notes: (a) Conventional; (b) canard; (c) tandem wing

Figure 2 Quickie Q2 (photographed by Adrian Pingstone in July 2005), scaled composites' unique tandem-wing proteus was tested for a series of UAV collision-avoidance flight demonstrations, ATTT133 – Rutan's the most famous aircraft in tandem-wing configuration ATTT

Note: Courtesy of Scaled Composites, LLC

Figure 3 Layout of the tandem-wing configuration

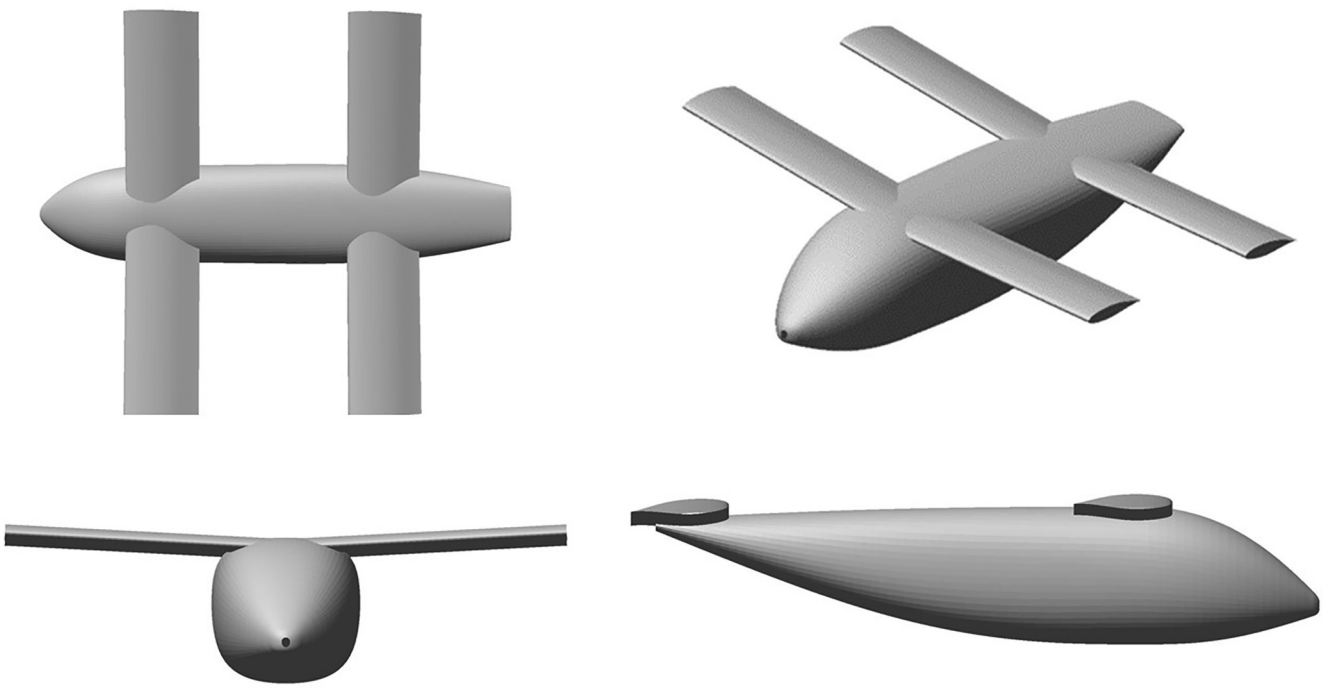

The following references were used during aerodynamic analysis of the aircraft:

- The front and rear wings have the same wingspan b = 5.4 m.
- The constant chord is equal to c = 1.0 m for both wings.
- The reference area is a sum of top view projection *t* of the front and rear wings' area and equal to A = 10.8 m^2.
- The position of the reference point was assumed in the half distant between 25% of the chord of the front and rear wings (Figure 4).
- Wing stagger referred to the wing chord is equal Δs = 1.5 (Figure 4).

The prepared model of aircraft was equipped with two independent control surfaces on the front and the rear wings.

Figure 4 Wings stagger definition and the reference point – CG

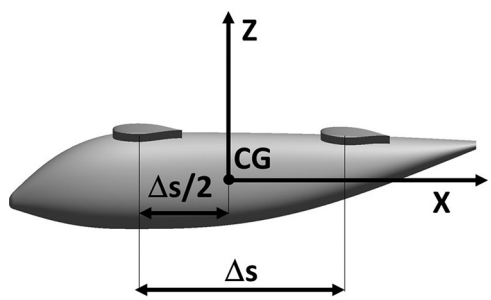

Figure 5 Front flap on the picture – left side, rear flap on the picture – right side

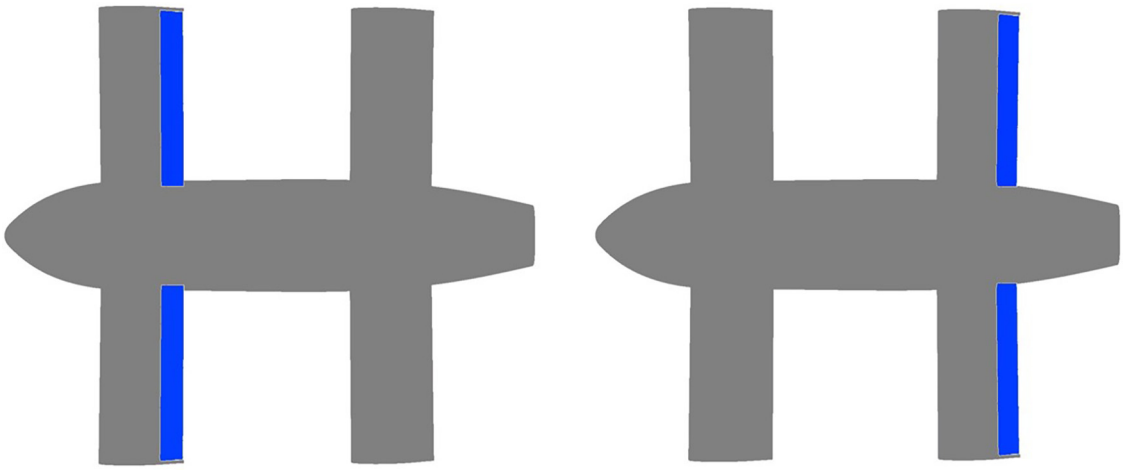

Both flaps are the same size (20% of MAC) and cover all wingspans, see Figure 5. The maximum deflection used during the analysis of each flap is limited to ±30 deg.

Numerical model

A numerical method for computation uses a model consisting of the fuselage and the front and the rear wings. To compute the aerodynamic impact, the MGAERO (MGAERO, 2001) software was used. This software used the Euler code with multigrid acceleration in the computation of the aerodynamic coefficients of arbitrary configuration (Mavriplis, 1992). Figure 6 presents the multigrid strategy for the aircraft with special attention to the wings.

The computing fluid dynamics (CFD) model consists of Multigrid Blocks: 8 levels and Surface mesh (Figure 6). They consist of 8,200 on body panels and 1,856,151 off-body panels. The deflection of flaps (front and the rear flaps) was modelled by a panel normal rotation (MGAERO, 2001).

Methodology

To define the longitudinal control strategy, firstly, a basic aerodynamic analysis of the considered configuration was made. As result, the aerodynamic coefficients versus angle of attack (AoA) were obtained. Special attention was paid to the distribution of aerodynamic loads on the front and the rear wings. The aerodynamic coefficients breakdown for the front and rear wings was researched. Such an analysis made it possible to determine aerodynamic coefficients and to build an aerodynamic model of the aircraft necessary to the analysis of trim conditions. The next important investigation was devoted to the analysis of the aerodynamic impact of the control surfaces deflection on the other aircraft's parts. To do this the CFD analysis (Anderson and Wendt, 1995) was made for independently deflected flaps placed on the front and rear wings.

All aerodynamic data obtained by CFD computations were used to build the analytical model of the aircraft longitudinal characteristics involving three basic equations:

Figure 6 Multigrid blocks and surface (on body) mesh

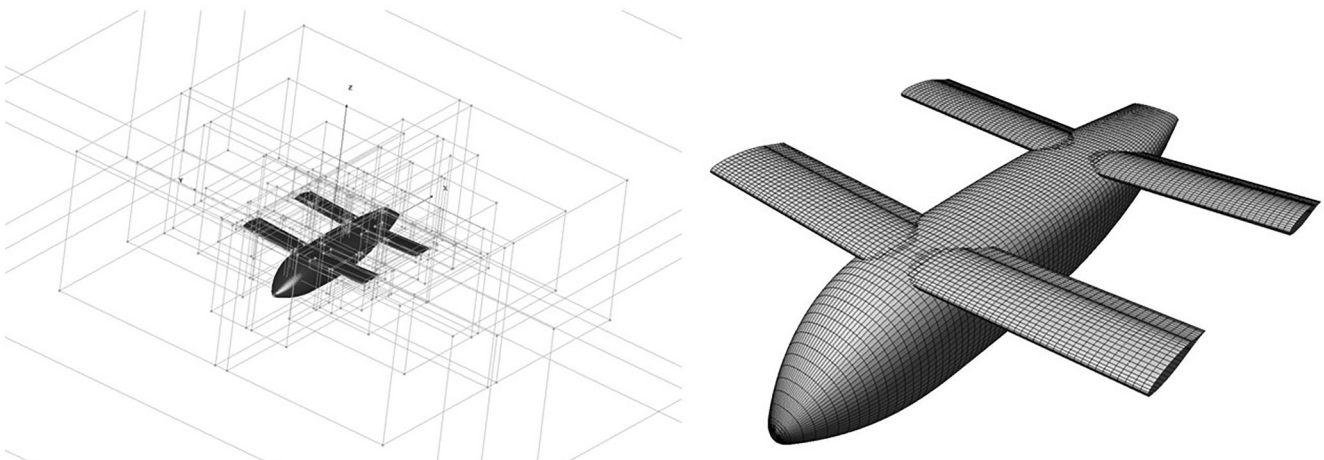

(a) (b)

$$\text{Lift coefficient } C_{L\,TOTAL} = f(\alpha, \delta_F, \delta_R)$$

$$\text{Drag coefficient } C_{D\,TOTAL} = f(\alpha, \delta_F, \delta_R)$$

$$\text{Pitching moment coefficient } C_{M\,TOTAL} = f(\alpha, \delta_F, \delta_R)$$

The main goal of the longitudinal control strategy is to find the best L/D ratio which satisfies the trim condition obtained by using both flaps. To obtained the solution, the optimisation method was used. The optimisation algorithm was based on the steepest descent method which belongs to the deterministic gradient method (Nocedal and Wright, 2006; Mieloszyk, 2017). To solve this problem, two different optimisations were done using different objective functions. The first one, F^1_{OBJ}, assumed to search the trim condition by two independent flaps deflection. So, the function includes only the pitching moment modulus, equation (1). So, the main goal was to find the minimum value of the pitching moment:

$$Minimise\ F^1_{OBJ} = |C_M| \tag{1}$$

The second objective function is an expansion of the previous function. Apart from the pitching moment coefficient includes the inverse form of L/D ratio too. It means that the deflection satisfied both the trim condition and maximum possible L/D ratio The definition is expressed by equation (2):

$$Minimise\ F^2_{OBJ} = |C_M| + \frac{D}{L} \tag{2}$$

the independent variables are presented below:

- δ_F deflection angle of the front wing flap; and
- δ_R deflection angle of the rear wing flap;

Results of computing fluid dynamics computation

As was mentioned, the first part of computation was devoted directly to finding the aerodynamic characteristics of the tandem wing in the clean configuration with special emphasis on both wing loads distribution. Figure 7 presents the exampled Cp distribution on the analysed aircraft. The

Figure 7 Cp distribution on the considered aircraft in tandem wing configuration

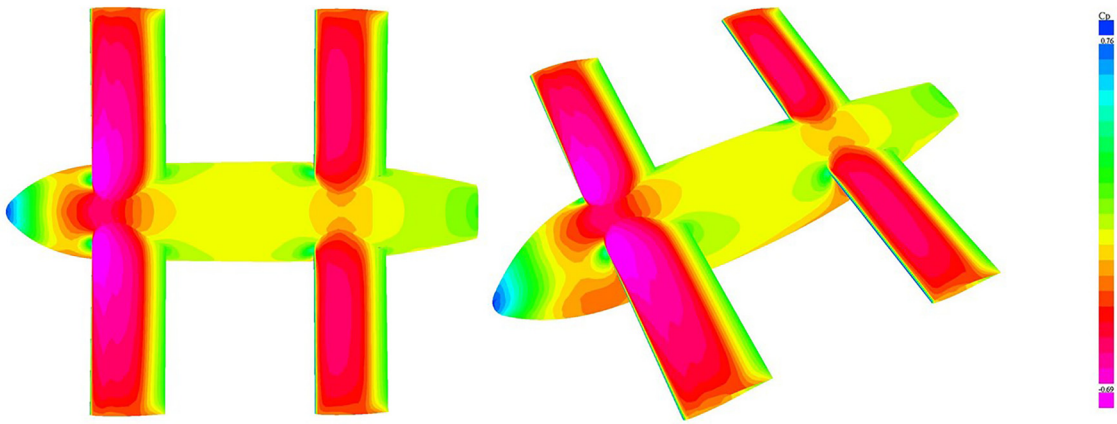

Figure 8 Lift coefficient breakdown

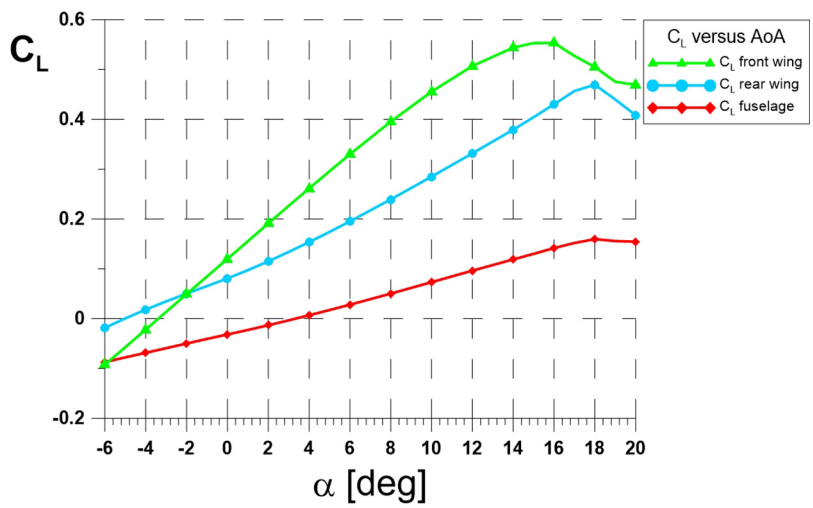

Notes: All presented results are referred to the same reference area.

qualitative analysis of the results reveals a significant reduction of the load on the rear wing caused by the front wing.

Quantified results of all analyses are presented in Figures 8, 10 and 11. First of all, the lift force coefficient versus AoA for the front, the rear wing and fuselage are presented (Figure 8). A significant difference between the wings lift force was observed. It was caused by the significant impact of the front wing. The lift force generated on the rear wing is lower than by the front despite the greater incidence angle. Moreover, meaningful changes in the lift slope, maximum lift force and critical AoA may be observed.

Next, the analysis of the pitching moment was made (Figure 9). It reveals that the configuration is statically unstable [Figure 9(a)]. As was expected, the front wing has a negative impact but a rear positive impact in the aircraft static stability. Unfortunately, the negative impact is higher [Figure 9(b)]. The pitching moment was referred to the reference point that is located exactly between the front and rear wings.

Finally, the drag coefficient breakdown was made (Figure 10). Generally, the rear wing contributes much more to the drag of the aircraft. The minimum drag of the rear wing was shifted back with respect to the front wing. It is caused by the difference in the incidence angle of the rear wing.

Verification of the computing fluid dynamics method

To verify the established CFD method (MGAERO, 2001), a second numerical software (low order method) was used. Verification was made by the panel method (Katz and Plotkin, 1991) implemented in Panukl software (PANUKL, 2022; Goetzendorf-Grabowski and Mieloszyk, 2017; Kwiek, 2018). The necessary model was built which consists of 5,098 body panels and 1,620 wake panels. All references like area, MAC and Centre of Gravity are the same as in the previous model, which was built for the MGAERO software. Wakes models, shaded from the front and the rear wings trailing edge are coupled with a free stream velocity direction. Free stream velocity was established as 36 m/s. Computation was made for AoA from −5 to 15 deg for clean configuration only. Figure 11 presents the grid model used for computation and Cp distribution for AoA 0 deg.

Figure 9 (a) Total pitching moment and (b) pitching moment breakdown

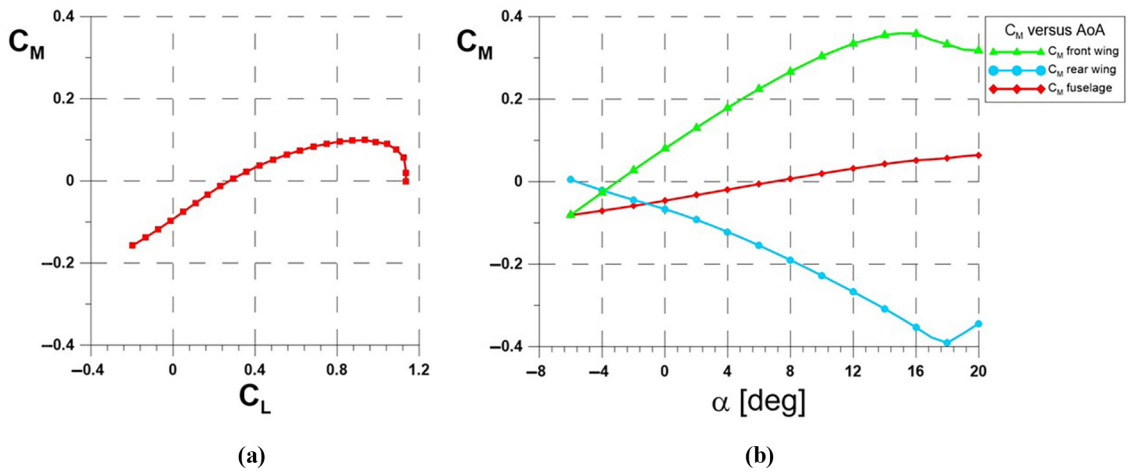

Figure 10 Drag coefficient breakdown

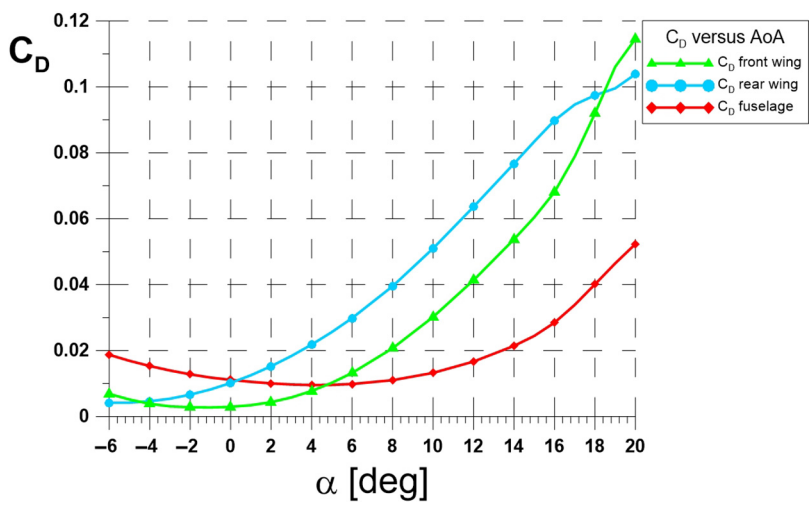

Figure 11 Model of the aircraft's mesh (on the left) and Cp distribution (on the right)

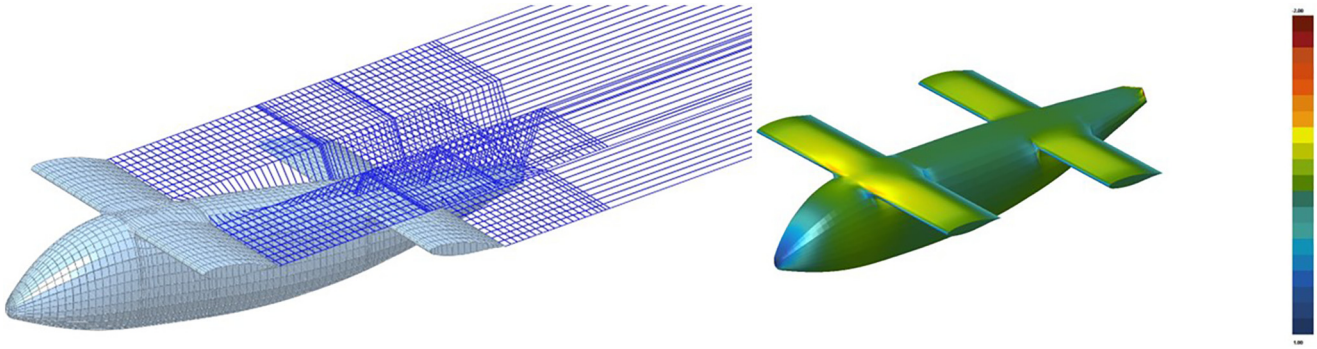

Figure 12 Comparison of the lift coefficient for the front and the rear wings

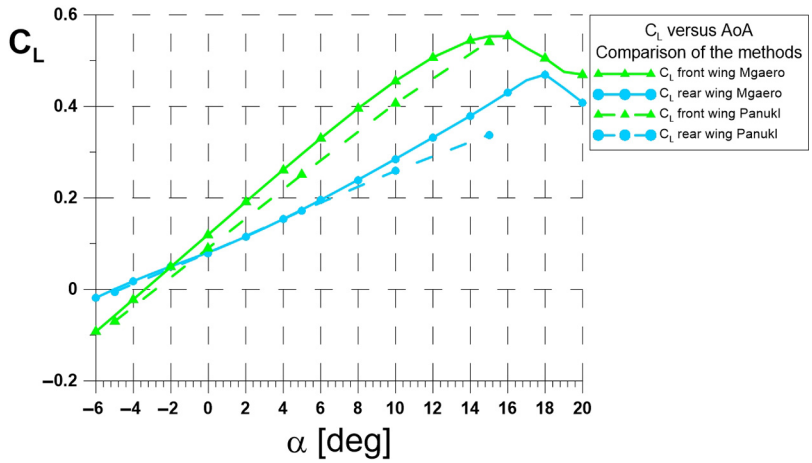

Next, the results of computation were compared with earlier obtained results by the MGAERO. Figure 12 presents the lift coefficient generated by the front (the green curve) and rear wings (the blue curve).

Results obtained for both wings are comparable with the coefficient obtained by the MGAERO software. The distribution of the lift coefficient obtained by Panukl software is linear in comparison with the front wing lift obtained by MGAER which is non-linear significantly. The small difference in results is caused by the impact of the rear wing on the front. This phenomenon is better represented by the MGAERO software.

Results for the rear wing are similar but for AoA less than 10 deg (Figure 12). For higher AoA, the rear wing performance depends on the front wing wake model. Wakes significantly reduce the lift on the rear wing. Its position with respect to the rear wing and shape significantly influence the lift generated on the rear wing. In this case, the MGAERO models the phenomenon more precisely. The wake impact on the rear wing lift makes it more non-linear.

A comparison of the two methods reveals that the results obtained by the MGAERO are acceptable for further analysis.

Front wing impact investigation (for clean configuration)

Further analysis was completely dedicated to computing and evaluating the front wing impact on the rear wing only. Another model was built to address this problem. The model [Figure 13(a)] used for computation is the same, but the front wing was removed. Moreover, all references necessary for analysis was the same. Figure 13(a) and 13(b) presents a comparison of the Cp distribution for the complete model of the aircraft and without the front wing. The qualitative analysis reveals significant change on the rear wing (left side) caused by the front wing influence.

The quantitative analysis is presented in Figure 14(a) and 14(b). A significant reduction in lift force for medium AoA was observed when the front wing is present. It influences the lift slope too. For low AoA, the lift slope was reduced but for higher angles increased. The rear wing achieves a similar maximum lift but for a higher value of the AoA [Figure 14(a)]. Figure 14(b) presents the comparison of the drag. The most important observation is that the rear wing generates a lower drag coefficient when the front wing is present. It is one of the features of tandem wing configurations.

Results of computation, especially the lift generated on the rear wing (when the front wing is not present), was compared with the lift generated on the rear wing in the complete model. It allowed to compute the downwash angle which is responsible for the mentioned lift reduction, see Figure 15(a). Further analysis, allowed to determine the change in the lift coefficient caused by the front wing [Figure 15(b)].

Figure 13 Cp distribution for the aircraft in tandem wing configuration – comparison of the CP distribution for a case (b) with and (a) without front wing impact

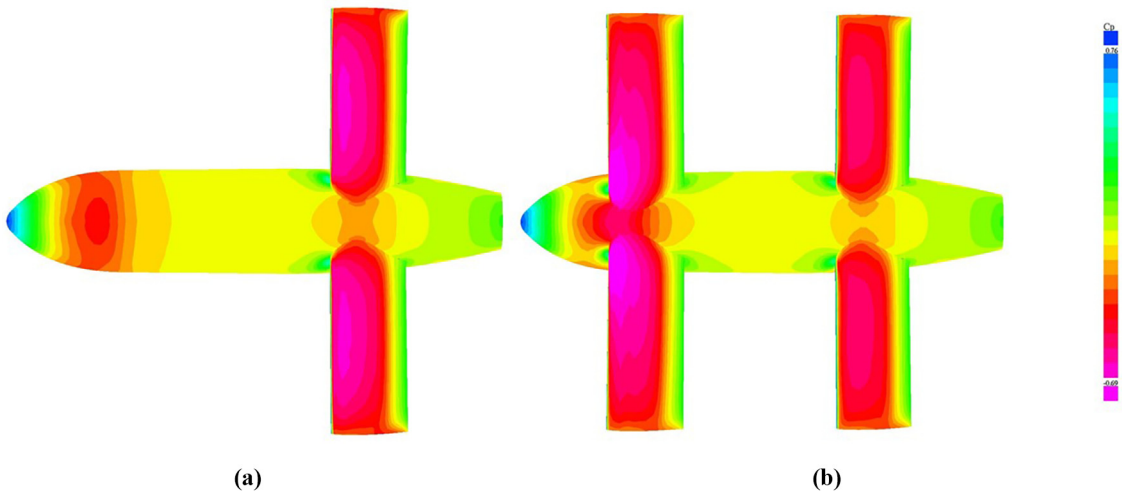

Figure 14 (a) Lift and (b) drag coefficients generated on the rear wing with impact front wing (red) and without impact front wing the rear (green) wing

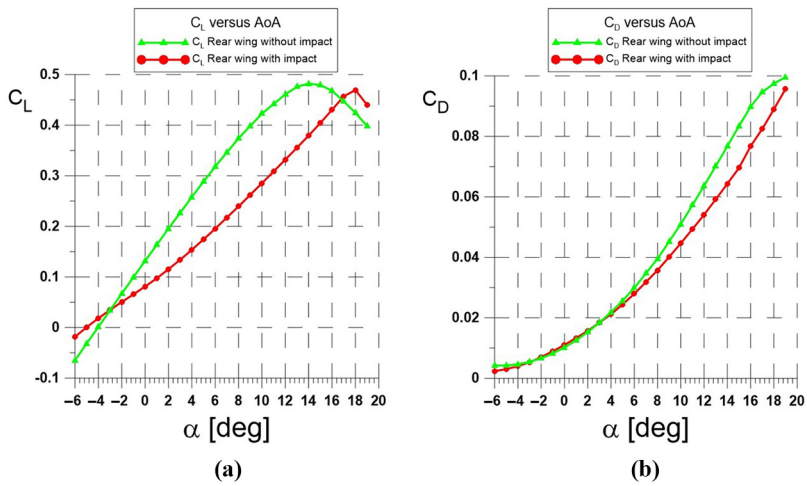

Figure 15 (a) Downwash angle and (b) reduction of the lift

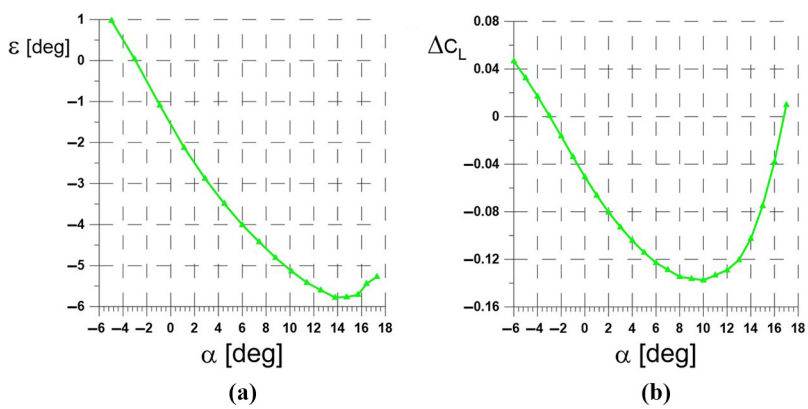

Aerodynamic impact of the flap deflection

The next part of this research was to find the impact of the flap deflection on the aircraft aerodynamic coefficients. The typical impact of the control surfaces was expected mainly on the lift force. But analysis of the numerical results showed that for the tandem wing configuration, this impact is much more complex. First of all, the impact of each flap deflection was studied independently. It means that when the front flap was deflected then the rear was undeflected and vice versa. In this way, the influence of flap deflections was determined. Analysis was made for a single AoA. The results of the computation are presented in Figure 16, which shows the Cp distribution on both wings after the rear flap was deflected.

The data obtained from the analysis were used to build the flaps impact model. Results of the lift forces and pitching moment were modelled by derivatives and analytical function (Table 1 and 2).

Two types of control derivatives were considered (Table 1). The first one was the derivative of the lift increment on a single wing (front or rear) in respect to deflection of the flap located on that wing. Similar values of derivatives were obtained. It was caused by using the same geometry of the wings and the flaps.

The second set includes the impact derivative of the lift increment on the wing caused by the deflection of the flap but on the other wing. The front flap deflection has a much

Figure 16 Cp distribution after (a) front flap and (b) rear flap deflection $\delta R = 20$ deg

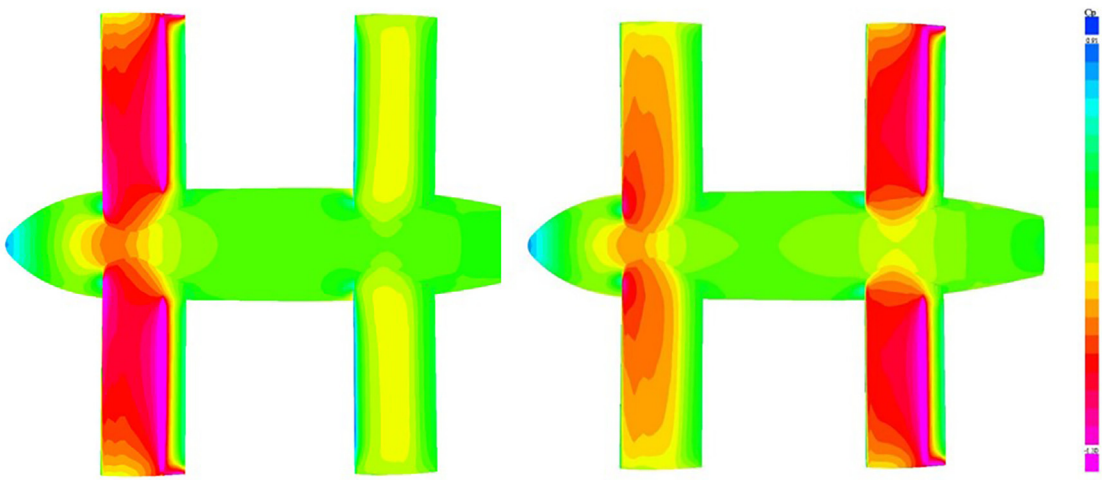

Table 1 Aerodynamic impact of flaps deflection on the lift coefficient

Derivative name	Symbol	Value
Front wing lift increment versus front flap deflection	$\frac{\partial C_{L,F}}{\partial \delta_F}$	0.875 [1/rad]
Rear wing lift increment versus front flap deflection	$\frac{\partial C_{L,R}}{\partial \delta_F}$	−0.375 [1/rad]
Front wing lift increment versus rear flap deflection	$\frac{\partial C_{L,R}}{\partial \delta_F}$	0.047 [1/rad]
Rear wing lift increment versus rear flap deflection	$\frac{\partial C_{L,R}}{\partial \delta_R}$	0.838 [1/rad]

Table 2 Aerodynamic impact of flaps deflection on the pitching moment coefficient

Derivative name	Symbol	Value
Front wing pitching moment increment versus front flap deflection	$\frac{\partial C_{M,F}}{\partial \delta_F}$	0.565 [1/rad]
Rear wing pitching moment increment versus front flap deflection	$\frac{\partial C_{M,R}}{\partial \delta_F}$	0.274 [1/rad]
Front wing pitching moment increment versus front flap deflection	$\frac{\partial C_{M,R}}{\partial \delta_F}$	0.033 [1/rad]
Rear wing pitching moment increment versus rear flap deflection	$\frac{\partial C_{M,R}}{\partial \delta_R}$	−0.692 [1/rad]

greater influence on the rear wing lift coefficient. Moreover, it contributes to a significant reduction of the lift force on the rear wing (the negative sign of the derivative $\frac{\partial C_{M,R}}{\partial \delta_R}$). The influence of the rear flap deflection on the front wing is rather low

Table 2 presents the pitching moment derivatives with respect to the deflection of the flap. Division on the two types of derivatives is the same as for lift derivatives. The front flap generates a positive increment of pitching moment but the rear flap negative. Other derivatives have rather minor impact, but it needs to be highlighted that again the front flap impact is observed. All these derivatives have a big influence on the trim condition.

Finally, the drag coefficient increment caused by flaps deflection was investigated. The CFD analysis reveals that this impact cannot be neglected, as it usually can be ignored for a conventional configuration. Moreover, for the tandem wing configuration, the impact significantly depends on the AoA too. The detailed analysis of the drag breakdown reveals that increment may be divided into three parts:

1 the drag force increment caused by the flap deflection on the front and rear wings (Figure 17);
2 the drag force increment on the rear wing caused by the front wing flap deflection (Figure 17); and
3 the drag force increment on the rear wing caused by the AoA change (Figure 18).

The analysis of the drag increment reveals a typical solution for this case (Figure 17). It is natural that drag increases after flap deflection (the front wing and the front flap). It was observed that for the rear flap deflection on the rear wing, the drag decreased for low flap deflection. It was caused by the front wing impact which reduced the lift on the rear wing. But the impact of the front flap deflection on the rear wing gets opposite results. The increase in drag increment is decreasing. It is caused by a significant reduction of the lift force generated on the rear wing by the front flap deflection, which reduces the drag increment.

Figure 17 Drag coefficient increment versus flaps deflection

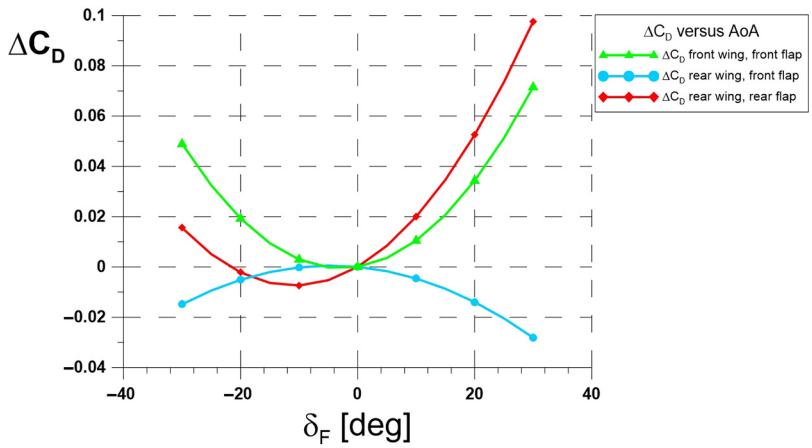

Figure 18 Drag coefficient increment caused by flap deflection versus AoA

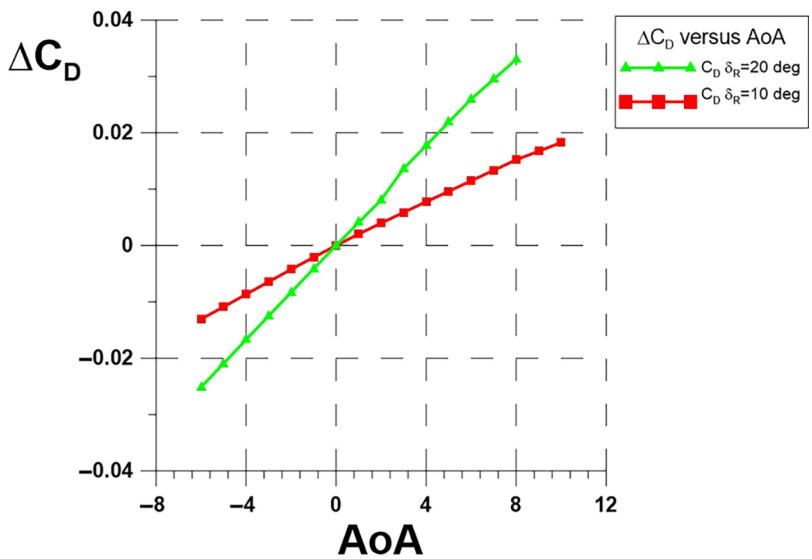

Trim condition

To find the trim condition of the aircraft, the system of three equations should be solved (Methodology). The equations describing the lift force, drag force and pitching moment of the complete aircraft must be derived. It was assumed that to satisfy the trim condition both flaps (front and rear) were used. Therefore, as the independent variables, the flaps deflection of the front and the rear wings were chosen. The solutions to the problem were obtained by the optimisation process described earlier. Computations were made for two different objective functions: F^1_{OBJ} and F^2_{OBJ}. The definition of those functions was presented earlier.

The first computation was made for the objective function F^1_{OBJ}. Figure 19(a) presents the necessary deflection of the front and rear flaps, which are results of the optimisation process. The deflection of both flaps is almost symmetrical. It means, that for the negative deflection of the front flap, the rear flap is positively deflected with almost the same deflection angle. Next, the L/D ratio was analysed [Figure 19(b)]. Application of the deflection of the flap, necessary to trim condition reveals that maximum L/D ratio was slightly reduced for the medium AoA in respect to the clean configuration.

Next, the static stability analysis was limited to analysis of the change in the pitching moment coefficient with respect to the AoA (Figure 20). The analysis was made for flaps deflection (from previous analysis), which assures the maximum L/D ratio. The analysis reveals that the configuration, for the assumed reference point, is unstable. Moreover, the analysed configuration was compared with the clean configuration (Figure 20 – red curve). The flap deflection does not improve the issue with the static stability of the aircraft but affected the pitching moment value.

Figure 19 Front and rear flap deflection

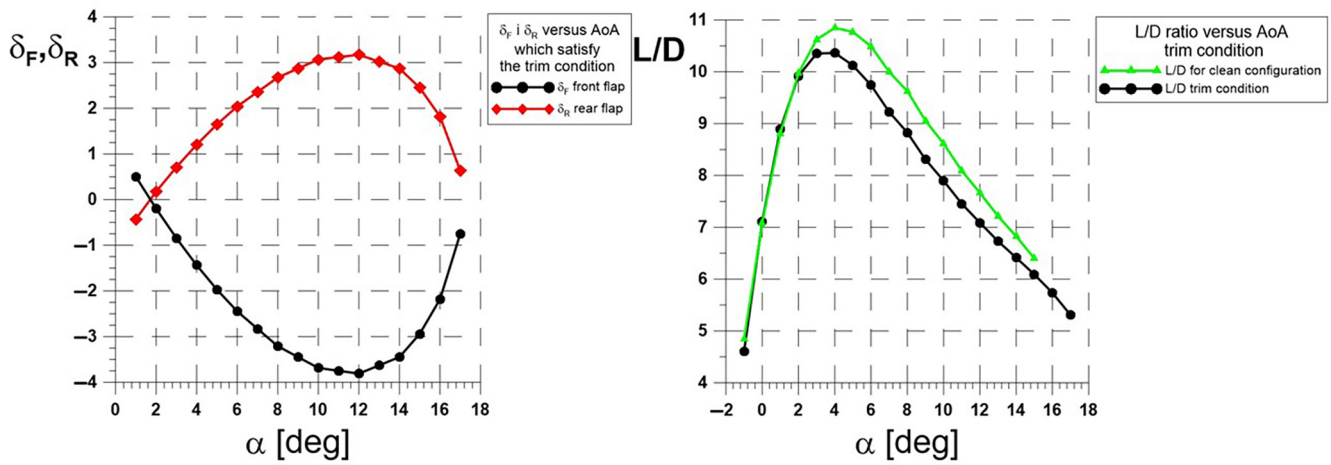

Notes: (a) Necessary to satisfy the trim condition and L/D ratio; (b) objective function F^1_{OBJ}

Figure 20 Pitching moment coefficient versus AoA – objective function F^1_{OBJ}

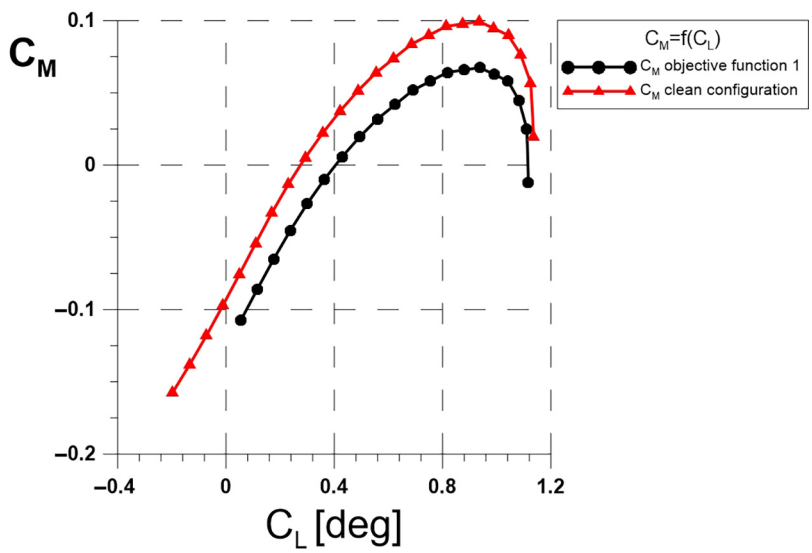

Figure 21 Front and the rear flap deflection

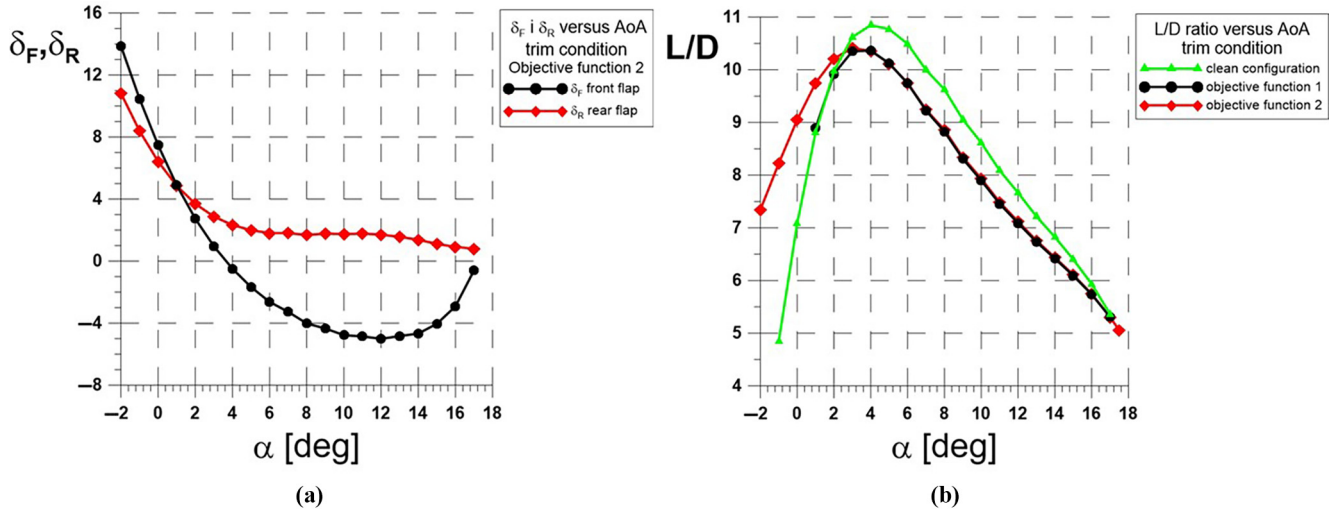

Notes: (a) Necessary to satisfy the trim condition and L/D ratio; (b) obtained for the objective function F^2_{OBJ}

The next set of the data were obtained for the objective functionF^2_{OBJ}. The flaps deflection was searched which satisfies the maximum L/D ratio. Figure 21(a) presents the result of both flaps deflection. The deflection is quite different than obtained for the previous analysis. Both flaps must be deflected by a positive angle (both increasing the lift) and the deflection angle is greater, up to 15 degrees. Moreover, the resulting L/D ratio curve was compared with the clean configuration and the previous computation [Figure 21(b)]. A significant difference in results between the first and the second objective functions was noticed; this may be observed in the value of L/D ratio for an AoA equal up to 4 deg. This range corresponds to a typical cruise condition. The second optimisation significantly increases the L/D ratio in the mentioned range of AoA.

Moreover, Figure 22 presents the comparison of the lift coefficient obtained for different flap deflection versus AoA, which satisfies the trim condition. The most important finding is the significant difference existing in the lift for low angles of attack. While for higher angles of attack, the lift curve is similar.

Finally, the comparison of the impact of flap deflection on the pitching moment was considered. Presented results satisfy the trim condition described in Figure 21. Figure 23 presents the comparison of the clean configuration and results obtained by the optimisation process for F^1_{OBJ} andF^2_{OBJ}. First of all, both

Figure 22 Lit coefficient CL versus angle of attack for clean configuration and configuration obtained for objective functions F^1_{OBJ} and F^2_{OBJ}, under the trim condition

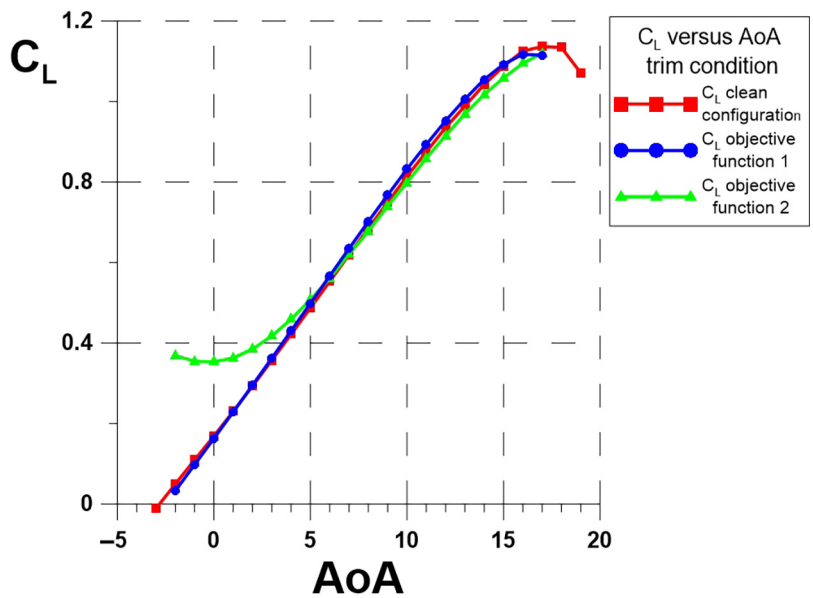

Figure 23 Comparison of the pitching moment versus lift coefficient

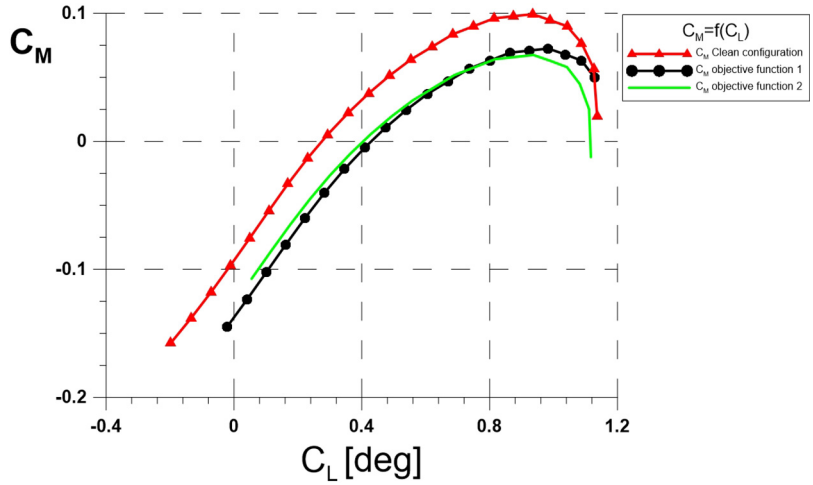

Figure 24 Comparison of the flap deflection δF and δR versus AoA for results obtained by objective function – F^1_{OBJ} and F^2_{OBJ}

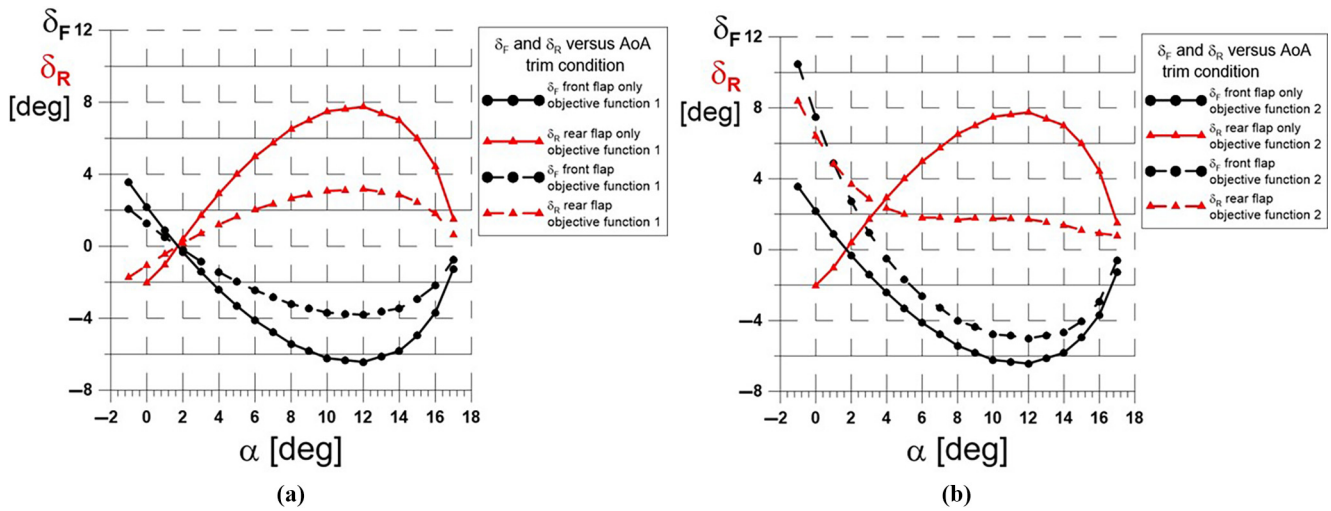

results for F^1_{OBJ} and F^2_{OBJ} do not improve the stability issue. Moreover, results for F^2_{OBJ} worsens the stability for the low AoA and improves for higher AoA with respect to the results obtained forF^1_{OBJ}.

Flap effectiveness investigation

To assess the aerodynamic effectiveness of each flap, the analysis of deflection that engage only the front flap or only the rear flap was made. In other words, the trim condition was satisfied but only by using one pair of flaps, the front or the rear. Figure 24 presents the deflection of the resulting flap that corresponds to the trim condition. The obtained deflection was next compared with the case when both flaps were used simultaneously; Figure 24(a) presents a comparison with the result of solving the objective function F^1_{OBJ} , and Figure 24(b) presents the comparison with of solving the objective functionF^2_{OBJ}.

Figure 25 Comparison of L/D ratio for both flaps deflection and flaps deflected separately

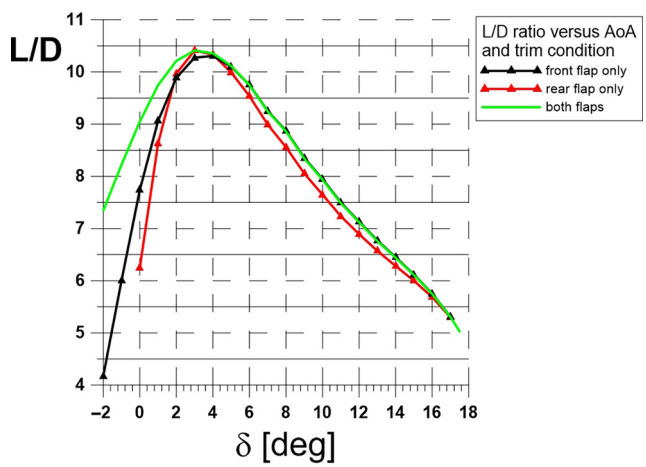

The comparison of the results presented in Figure 24(a), when only the front or only the rear flap is used, shows that the deflection must be significantly greater to satisfy trim conditions. Moreover, the curves of necessary deflections are similar to the result obtained for deflection of both flaps simultaneously. In the case of Figure 24(b), the rear flap deflection shape is completely different but the front flap trend is similar. It is caused by the higher impact of the front flap on the rear flap.

Finally, Figure 25 presents a comparison of the L/D ratio for the scenario when only the front flap is deflected and when only the rear flap is deflected. Moreover, both results are compared with the case when both flaps were used simultaneously. The presented analysis shows the effectiveness of the rear flap is higher. It means that for a trim condition, a higher value of the L/D ratio can be obtained.

Summary and conclusions

In this paper, the aerodynamic analysis for the designed aircraft in tandem wing configuration is presented. The main goal of research was to determine the possible benefits of the tandem wing with the emphasis on aerodynamics. Typically for unconventional configurations a challenge is to keep a good aerodynamic performance but under the trim condition. To address the research question, firstly, numerical aerodynamic computation were used to establish the mutual impact of the front and rear wings. Then, analysis with independently deflected flaps was conducted. Based on collected data a numerical model were built, which was implemented in the numerical optimisation. The aim of this optimisation process was to find the optimal flaps deflection which allows to obtain the aircraft's maximum L/D ratio under trim condition.

As was expected, the CFD analysis reveals that the front wing has a significant impact on the rear wing. This causes a major reduction of the lift on the rear wing and impacts the value of the pitching moment. The downwash angle was used in quantified analysis of the front wing impact on the rear wing. Moreover, the analysis devoted to flaps deflection reveals the significant impact of the front flap on the rear wing.

Results of all analyses confirm that the tandem wing configuration is strongly aerodynamic coupled. The wings arrangement (wing stagger) plays important role for the clean configuration aerodynamics, but in case of the considered configuration, the impact of the control surfaces deflection cannot be neglected. The research showed that the trim condition may be obtained for different flaps deflections. Moreover, it may be obtained only by a single deflection of flap (only front or only rear). But, it does not guarantee to obtain the maximum possible L/D ratio. The application of the proper flaps deflection is the key to achieve the best aircraft's L/D ratio under the trim condition. And it may be obtained by the optimisation process only, what was showed in this paper.

The strong coupled aerodynamic configuration like a tandem wings is a very complex problem. Therefore all obtained results should be verified by the wind tunnel tests or during flight tests campaign.

References

Anderson, J.D. and Wendt, J. (1995), *Computational Fluid Dynamics*, Vol. 206, McGraw-Hill, New York, NY, p. 332.

Brinkworth, B.J. (2016), "On the aerodynamics of the miles libellula tandem-wing aircraft concept", *Journal of Aeronautical History Paper*, Vol. 2, pp. 1941-1947.

Cheng, H., Shi, Q., Wang, H., Shan, W. and Zeng, T. (2021), "Flight dynamics modeling and stability analysis of a tube-launched tandem wing aerial vehicle during the deploying process", *Proceedings of the Institution of Mechanical Engineers, Part G: Journal of Aerospace Engineering*, doi: 10.1177/09544100211010903.

Chou, H.Y., Liu, Y.C. and Hsiao, F.B. (2013), "The aerodynamic behavioral study of two wing's wake flow in tandem arrangement", *Procedia Engineering*, Vol. 67, pp. 1-14, doi: 10.1016/j.proeng.2013.12.001.

Chudoba, B. (2019), "Stability and control of conventional and unconventional aerospace vehicle configurations", Springer ISBN: 978-3-030-16855-1.

Goetzendorf-Grabowski, T. and Antoniewski, T. (2016), "Three surface aircraft (TSA) configuration – flying qualities evaluation", *Aircraft Engineering and Aerospace Technology*, Vol. 88 No. 2, pp. 277-284.

Goetzendorf-Grabowski, T. and Figat, M. (2017), "Aerodynamic and stability analysis of personal vehicle in tandem-wing configuration", *Proceedings of the Institution of Mechanical Engineers, Part G: Journal of Aerospace Engineering*, Vol. 231 No. 11, pp. 2146-2162.

Goetzendorf-Grabowski, T. and Goraj, Z. (1987), "Lateral stability of canard configuration", *Journal of Theoretical and Applied Mechanics*, Vol. 25 Nos 1/2, pp. 47-61.

Goetzendorf-Grabowski, T. and Mieloszyk, J. (2016), "Unconventional configurations – design and optimization", *Proceedings of 30th International Congress Of The Aeronautical Sciences*, ICAS 2016-0067, *Deajeon 2016, ISBN: 978-3-932182-85-3*, pp. 1-8.

Goetzendorf-Grabowski, T. and Mieloszyk, J. (2017), "Common computational model for coupling panel method with finite element method", *Aircraft Engineering and Aerospace Technology*, Vol. 89 No. 5, pp. 654-662, doi: 10.1108/AEAT-01-2017-0044.

Goraj, Z. (2014), "Flight dynamics models used in different national and international projects", *Aircraft Engineering and Aerospace Technology*, Vol. 86 No. 3, p. 3.

Gudmundsson, S. (2014), *General Aviation Aircraft Design*, Butterworth-Heinemann,Oxford.

Hallion, R.P. (2019), *The Wright Flyers 1899–1916: The Kites, Gliders, and Aircraft That Launched the "Air Age"*, Bloomsbury Publishing, London.

Jones, R., Cleaver, D. and Gursul, I. (2015), "Aerodynamics of biplane and tandem wings at low reynolds numbers", *Experiments in Fluids*, Vol. 56 No. 6, doi: 10.1007/s00348-015-1998-3.

Katz, J. and Plotkin, A. (1991), *Low-Speed Aerodynamics, from Wing Theory to Panel Methods*, McGraw-Hill, New York, NY.

Kundu, A.K., Price, M.A. and Riordan, D. (2019), *Aircraft Design*, John Wiley & Sons, Hoboken, 8 kwi 2019 – 1056

Kwiek, A. (2016), "Study on the static and dynamic stability of a modular airplane system", *Aviation*, Vol. 20 No. 4, pp. 160-167.
Kwiek, A. (2018), "A numerical study into the longitudinal dynamic stability of the tailless aircraft", *Aircraft Engineering and Aerospace Technology*, Vol. 91 No. 3, pp. 428-436.
Mavriplis, D.J. (1992), "Three-dimensional unstructured multigrid for the euler equations", *Journal of Aircraft*, Vol. 30 No. 7, pp. 1753-1761.
MGAERO (2001), "A cartesian multigrid euler code for flow Around arbitrary Configurations – User's manual version 3.1.4",
Mieloszyk, J. (2017), "Practical problems of numerical optimization in aerospace sciences", *Aircraft Engineering and Aerospace Technology*, Vol. 89 No. 4, pp. 570-578.
Munk, M.M. (1922), "General biplane theory", NACA.
Nelson, R.C. (1998), *Flight Stability and Automatic Control*, 2th ed., McGraw-Hill, New York, NY.
Nocedal, J. and Wright, S. (2006), *Numerical Optimization*, Springer Science & Business Media, Berlin.
PANUKL (2022), available at: www.meil.pw.edu.pl/add/ADD/Teaching/Software/PANUKL
Phillips, W.F. (2004), *Mechanics of Flight*, John Wiley & Sons, Hoboken.
Proteus (2021), available at: www.scaled.com/projects/proteus
Rizzi, P., Goetzendorf-Grabowski, T., Vos, J.B., Zhang, M. and Richardson, T.S. (2011), "Design of a canard configured TransCruiser using CEASIOM", *Progress in Aerospace Sciences*, Vol. 47 No. 8, pp. 695-705.
Roedts, R. (2009), "Design of a biplane wing for small-scale aircraft", *47th AIAA Aerospace Sciences Meeting including the New Horizons Forum and Aerospace Exposition*, doi: 10.2514/6.2009-207.
Roskam, J. and Lan, C.T.E. (1997), *Airplane Aerodynamics and Performance*, DARcorporation, St, Lawrence, KS.
Schmitt, D. (2001), "Challenges for unconventional transport aircraft configurations", *Air & Space Europe*, Vol. 3 Nos 3/4, pp. 67-72. ISSN 1290-0958.
Scholz, D. (2015), "Aircraft design", Hamburg University of Applied Sciences, document available at: www.fzt.haw-hamburg.de/pers/Scholz/HOOU/
Stinton, D. (2001), *Design of the Aeroplane*, 2nd ed., Wiley-Blackwell, Hoboken.
Westin, M. and Pinto, R. (2008), "Wing-by-Wing approach for biplane static longitudinal stability and control analysis", doi: 10.13140/2.1.1179.7282.

Corresponding author

Marcin Figat can be contacted at: mfigat@meil.pw.edu.pl